ANTICANCER RESEARCH *40*: 6799-6815 (2020)
doi:10.21873/anticanres.14703

Anti-cancer Effects of Fucoxanthin on Human Glioblastoma Cell Line

FLAVIA GARCIA LOPES[1], KAREN ANDRINEIA OLIVEIRA[2], RAFAEL GARCIA LOPES[3], GABRIELA GODOY POLUCENO[2], CARMEN SIMIONI[4], GABRIEL DA SILVA PESCADOR[5], CLAUDIA MARLENE BAUER[6], MARCELO MARASCHIN[6], ROBERTO BIANCHINI DERNER[3], RICARDO CASTILHO GARCEZ[5], CARLA INES TASCA[2] and CLAUDIA BEATRIZ NEDEL[1,2]

[1]*Laboratório de Biologia Celular de Gliomas, Programa de Pós-Graduação em Biologia Celular e do Desenvolvimento, Universidade Federal de Santa Catarina, Florianópolis, SC, Brazil;*
[2]*Laboratório de Neuroquímica-4, Programa de Pós-Graduação em Bioquímica, Universidade Federal de Santa Catarina, Florianópolis, SC, Brazil;*
[3]*Laboratório de Cultivo de Algas, Universidade Federal de Santa Catarina, Florianópolis, SC, Brazil;*
[4]*Laboratório de Biologia Celular Vegetal, Programa de Pós-Graduação em Biologia Celular e do Desenvolvimento, Universidade Federal de Santa Catarina, Florianópolis, SC, Brazil;*
[5]*Laboratório de Células Tronco e Regeneração Tecidual, Programa de Pós-Graduação em Biologia Celular e do Desenvolvimento, Universidade Federal de Santa Catarina, Florianópolis, SC, Brazil;*
[6]*Laboratório de Morfogênese e Bioquímica Vegetal, Universidade Federal de Santa Catarina, Florianópolis, SC, Brazil*

Abstract. *Background/Aim: Glioblastomas (GBMs) are the most malignant primary brain tumor. New treatment strategies against the disease are urgently needed, as therapies are not completely efficient. In this study, we evaluated the antitumorigenic activity of the carotenoid fucoxanthin (Fx) on human GBM cells in vitro. Materials and Methods: GBM1 cell viability and proliferation was assessed by MTT reduction, Ki67 and single cell cloning assays. GBM1 migration and invasion were analyzed by wound healing and Transwell assays. Apoptosis and necrosis were analyzed by flow cytometry, and the mitochondrial membrane potential (ΔΨm) by the selective fluorescent dye tetramethylrhodamine ethyl ester. Cell morphology was analyzed through scanning electron microscopy and transmission electron microscopy. Fx anti-angiogenic effect was assessed by the CAM ex ovo assay. Results: Fx decreased cell viability in a concentration-dependent manner (40-100 μ M) in GBM1, A172 and C6 cell lines and was not cytotoxic to murine astrocytes. In addition, Fx inhibited the proliferation and clonogenic potential, and decreased migration and invasion of GBM1 cells. Furthermore, Fx induced apoptosis, loss of ΔΨm and ultrastructural alterations in GBM1. Fx-treated GBM1 cells-conditioned medium reduced the quail yolk membrane vascularity. Conclusion: Fx induces cytotoxicity, anti-proliferative, anti-invasive and anti-angiogenic effects on GBM1 cells.*

Correspondence to: Claudia Beatriz Nedel (ORCID ID 0000-0002-9075-8127), Laboratório de Biologia Celular de Gliomas, Universidade Federal de Santa Catarina, Trindade, Florianópolis, 88040-900, Santa Catarina, Brasil. Tel: +55 4837212629, e-mail: claudianedel@gmail.com

Key Words: Glioblastoma, fucoxanthin, apoptosis, migration, invasion, angiogenesis.

Gliomas are primary tumors that affect the central nervous system (CNS). The origin of glioma cells is not completely elucidated, and may derive from dedifferentiation of a mature cell type, glial progenitor cells or primitive neural stem cells (1). The primary malignant brain neoplasms global-gender incidence rate is approximately 2.6 per 100,000 for females and 3.7 per 100,000 for males, per year (2). Gliomas compose only 27% of all CNS primary neoplasms, however, it represents almost 80% of all malignant primary tumors that affect this system (3, 4).

Gliomas are histopathologically categorized by the World Health Organization (WHO) into different subtypes and grades (I to IV), as oligodendroglioma, oligoastrocytoma and astrocytoma. Grade IV is reserved for a subtype of astrocytoma, the glioblastoma (GBM) (5). GBM is the most malignant glioma and the most frequent primary cerebral tumor, with an incidence of 3.2 cases per 100,000 person/year

(6). Evidence also suggests that the incidence of GBM is ethnicity, gender and geographic/location–dependent. Studies indicate that GBM is 1.6 times more frequent in men than women (7, 8), and 2 to 3 times more prevalent among Caucasians than African American, American Indian, Alaskan native and Asian-Pacific islander populations (9).

GBMs are microscopically distinguished from the other types of gliomas by the presence of pathological microvascular proliferation and areas of necrosis, often surrounded with pleomorphic tumor cells in a pseudopalisading pattern (10).

Gliomas in general, specifically GBMs, are very difficult to treat. The standard treatment protocol for adult patients diagnosed with GBM is surgical resection followed by chemotherapy with Temozolomide (TMZ) and concomitant radiotherapy followed by TMZ (11, 12). Despite advances in diagnostic techniques and therapies, the GBM patient's survival rate is approximately 14 months (10, 13, 14).

The low survival rate and treatment inefficacy is related to the aggressive nature of GBM, which is caused by several key mechanisms including, evasion of apoptosis (15), migration and invasion into normal brain tissues and the induction of angiogenesis (16-19). Therefore, it is important to study treatment options that can suppress and prevent its tumorigenesis mechanisms.

Several effective anti-carcinogenic medications have been found in natural sources, but crucial unexplored resources remain to be investigated, the edible seaweeds and marine diatoms (20). Fucoxanthin (Fx) is a component of algae biomass, an abundant marine xanthophyll and the pigment responsible for providing seaweeds the typical brown color. Fx also represents over 10% of the total carotenoids found in nature (21).

This carotenoid displays diverse biological activities, including antioxidant (22), antidiabetic (23), anti-obesity (24), antimutagenic (25), anti-inflammatory (26), and anticancer effects (27) on leukemia, colon, lung, prostate, liver, gastric and neuroblastoma cancers (22, 28-34). Fx exerts its anticancer and anti-proliferative activity through diverse signaling pathways associated with metastasis, apoptosis, cell cycle arrest, and angiogenesis.

The use of natural compounds, such as Fx, with proven anticancer activity, which are present in a well-established diet, like the one found in regions with a low incidence of glioma, is a promising strategy for an alternative treatment for this type of tumor. Therefore, the main purpose of this study was to investigate the effects of Fx, extracted from the marine diatom *Phaeodactylum tricornutum,* on human GBM cells.

Materials and Methods

Fucoxanthin extraction. Batch cultures of *Phaeodactylum tricornutum* (CCAP 1055/1) were cultivated until the late exponential phase, and then, the biomass was centrifuged (3,000 g × 5 min), washed and freeze-dried. Fx was extracted from the biomass with MeOH, and the carotenoid extracts were further purified with ethyl acetate to separate the most polar phase. Lastly, to obtain a Fx rich fraction, a gel silica chromatography was employed following Takahashi (35). The fraction quantification was conducted by High-performance liquid chromatography (HPLC) and the Fx identity verified through mass spectrometry (LC-MS/MS).

Cell cultures. The human GBM sample was surgically resected from a patient at the Celso Ramos Hospital, in Florianopolis, Santa Catarina, Brazil. The sample collected was placed in a 15 ml conical tube containing Dulbecco's Modified Eagle's Medium and F12 nutrient mixture (DMEM-F12; Invitrogen, Carlsbad, CA, USA), with 10% fetal bovine serum (FBS; Cultilab, Campinas, SP, Brazil). In a laminar flow cabinet, the sample was dissected (cerebral membranes and blood vessels and were detached), dissociated with trypsin (Trypsin/EDTA, 0.05%; Invitrogen), washed with phosphate buffered saline (PBS) and plated in 25 cm^2 culture flasks, containing DMEM-F12 with 10% FBS, in culture conditions (atmosphere of 5% CO_2/95% air) at 37˚C. This cell culture was used for further experiments after the 10^{th} passage to assure that it did not contain non-specific cell types and was called GBM1. All experiments were approved by the local ethics committee for human research (CEPSH/UFSC 108.286). The primary astrocyte cultures were obtained from newborn (0 to 3-day-old) Wistar rats' cerebral cortex, as previously described (36). The astrocytes were seeded on 96-well plates (3.5×10^5 cells) containing DMEM-F12 with 10% FBS and cultivated for 10-14 days (80% confluence). The cell cultures were placed in an incubator, in a humidified atmosphere of 5% CO_2 and 95% air at 37˚C. These experiments were approved by the local ethics committee for animal research (CEUA/UFSC PP00955). The human glioma cell line A172 and murine glioma cell line C6 were cultivated in DMEM F-12 containing 10% FBS. The human umbilical vein endothelial cells (HUVECs) were kindly provided by Prof. Dr. Tânia Beatriz Creczynski Pasa (Department of Pharmaceutical Sciences, UFSC, CA, USA) and cultured in a RPMI 1640 medium (Invitrogen) containing 10% FBS. All cell lines were cultured in 25 cm^2 culture flasks at 37˚C in a humidified atmosphere of 5% CO_2 and 95% air. When 80% confluence was reached, the cells were trypsinized and plated in 24 and 96 well plates (1×10^4 cells/well).

During treatment, all groups, including control (CT), were cultured in a serum-free medium solution. GBM1, A172, C6 and murine astrocytes were treated with Fx at concentrations of 10, 40, 70, 100, and 150 μM, for 24 h. Vehicle-controls were incubated with the equal volume of dimethyl sulfoxide (DMSO, max of 0.1%; Vetec, Duque de Caxias, RJ, Brazil).

Cell viability assay. To analyze the Fx effect on cell viability (GBM1, A172 and C6 and murine astrocyte) the MTT assay was performed. As previously described (37), this experiment evaluates the cell's capacity to convert 3-(4,5-dimethylthiazol-2-yl)-2,5-diphenyltetrazolium bromide (MTT) to an insoluble purple formazan. After 24 h of treatment with 10, 40, 70, 100 or 150 μM Fx the culture medium was removed and replaced with the MTT solution (0.2 mg/ml in PBS; Sigma-Aldrich, St. Louis, MO, USA), followed by a 2 h incubation period at 37˚C. Then, DMSO was added to dissolve the formazan crystals. The viability was spectrophotometrically assessed with a multimode reader Infinite M200 TECAN, at a wavelength of 540 nm. Additionally, the number of cells exposed to Fx (40-70 μM) was quantified; after 24 h Fx treatment the cell nuclei were stained with Hoechst 33258 (5

μg/ml; Sigma-Aldrich) for 10 min, and images were obtained. Ten random fields were photographed per sample with an Olympus IX83 fluorescent microscope, and the cells were counted.

Cell proliferation assay. To analyze the Fx effect on GBM1 proliferation, a Ki-67 cell proliferation assay was carried out. First, cells were grown on sterile coverslips and after they reached confluency, were treated with 100 μM Fx for 24 h. After the treatment period, GBM1 cells were fixed with 4% paraformaldehyde (PFA) for 20 min and incubated overnight with Ki-67 antibody (1:500; Millipore, Burlington, MA, USA) at 4˚C, followed by a second incubation with anti-rabbit IgG secondary antibody conjugated with Alexa Fluor-488 (1:500; Abcam, Cambridge, UK) for 60 min at room temperature. Finally, cells were incubated with the Hoechst 33258 stain (5 μg/ml) for 10 min. Images were from ten random fields with a fluorescent microscope (Olympus IX83), and the cells were quantified. To establish the cell proliferation rate, the number of Ki-67-positive stained cells was divided by the total of Hoechst-stained cells. The experiment was executed three times independently with three replicates per group.

Single cell cloning by serial dilution assay. This assay was used to evaluate the effect of Fx on the clonogenic and replicative potential of a single GBM1 cell. First, GBM1 cells were plated in 24 well plates (1×10^4 cells/well), and after they reached confluency, were treated with 40, 70 or 100 μM Fx for 24 h. After the treatment period, the cells were rinsed with PBS, trypsinized and counted in a Neubauer chamber. A serial dilution of cells in DMEM-F12 was then performed. Next, approximately 1 cell per well (96-well plate) was seeded and cultured in DMEM F-12, supplemented with 10% FBS for 12 days in a humidified cell incubator. Photos were taken on days 2, 7 and 12 utilizing a 10 X objective lens in an inverted microscope (Zeiss Axiovert 40 CFL, capture system AxioCam MRc). At the twelfth day of incubation, the MTT assay was performed to quantify the number of clones. The number of clones was proportional to the absorbance, which was obtained using a spectrophotometer (Multimode Reader Infinite M200 TECAN) at a wavelength of 550 nm.

Wound healing assay. To analyze GBM1 cell mobility changes after Fx exposure, a wound-healing assay was performed as previously described (38, 39). First, GBM1 cells were seeded in 24-well plates; after they reached confluency, a straight line was made in the dish surface with a sterile pipette-200 tip. Afterwards, the medium was replaced with an FBS-free medium with different Fx concentrations (40-100 μ M). The cells were then stained with 10 μg/ml acridine orange (Sigma-Aldrich) for 10 min and photographed. Pictures were taken at 0 and 24 h using a 10 X objective lens of an inverted microscope (Zeiss Axiovert 40 CFL, capture system AxioCam MRc). The gap width was obtained by the average of 5 measurements from each scratch. Each measurement was calculated from the scratch's right edge to the left edge, beginning from the top to the base of the image using ImageJ® software.

In vitro migration assay. To analyze the effect of Fx on GBM1 cell mobility we performed the Transwell® (Corning, Tewksbury, MA, USA) migration assay as described previously (40). Briefly, GBM1 cells were placed on top of the Transwell®, with (40, 70 or 100 μM) or without Fx, and incubated at 37˚C and 5% CO_2 for 10 min. Next, the lower chamber of the 24-well plate was filled with a chemoattractant solution (20% FBS DMEM-F12). After 24 h, GBM1 cells located on the lower membrane surface were stained with Hoechst (5 μg/ml) and quantified using a fluorescence microscope (Olympus IX83).

In vitro invasion assay. The invasive potential of GBM1 cells after exposure to Fx was measured using a Transwell® insert coated with Matrigel®. First, 50 μl of Matrigel® (5 mg/ml; Corning) were placed on top of the Transwell® insert, and incubated for 30 min, for polymerization. Then, cells that were suspended in serum-free DMEM-F12 containing Fx, added to the upper compartment of the chamber and cultured for 10 min to allow cell sedimentation. Next, the chemoattractant solution containing DMEM-F12 and 20% FBS was added at the lower chamber and the plate was placed for 24 h at 37˚C in a humidified incubator with 5% CO_2. The cells located on the membrane's upper surface (non-invading cell), were detached with a cotton-tipped applicator. The invasive cells attached to the insert's lower membrane surface were stained with Hoechst (5 μg/ml) for 10 min and counted using a fluorescence microscope (Olympus IX83). The invaded cells were counted in 10 randomly chosen fields from each membrane.

Apoptosis and necrosis analysis. To evaluate the effect of Fx on GBM1 necrosis or apoptosis levels, the Annexin V-FITC assay kit (Millipore) was used and the analysis was performed by flow cytometry. Briefly, GBM1 cells were seeded in 24-well plates overnight and then treated with 100 μ M Fx for 24 h. Afterwards, as suggested by the manufacturer, GBM1 cells were trypsinized, centrifuged at 220 × g and rinsed twice in cold PBS. Next, cells were homogenized in a binding buffer (200 μl) and incubated with 5 μl of propidium iodide (PI, 5 μg/ml; Millipore) and 5 μl Annexin V-FITC at room temperature for 15 min. The cells were separated by a FACSCanto II flow cytometer and the results were analyzed using a Flowing Software 2. The nuclei morphology changes were analyzed by Hoechst 33258 nuclear staining (41). GBM1 cells were seeded on coverslips and after they reached confluence (overnight) were treated with 100 μM Fx for 24 h; the coverslips were then rinsed with PBS and fixed with PFA 4% for 20 min. Next, cells were incubated with Hoechst 33258 staining solution (5 μg/ml) for 10 min, washed with PBS and mounted on microscope slides. Images were taken using a fluorescent microscope (Olympus IX83) at an excitation wavelength of 340 nm.

Mitochondrial analysis. The selective fluorescent dye tetramethylrhodamine ethyl ester (TMRE) was used to evaluate the effect of Fx on GBM1 mitochondrial membrane potential. GBM1 cells were seeded into a 96-well plate, and after they reached confluence, were treated with Fx 100 μ M for 24 h. After treatment, GBM1 cells were loaded with TMRE (100 nM; Sigma-Aldrich) for 30 min at 37˚C (42). The mitochondrial uncoupler, carbonyl cyanide p-trifluoromethoxy phenylhydrazone (FCCP 20 μM; Sigma-Aldrich), was utilized as a positive control of fluorescence emission. The fluorescent intensity was determined by excitation at 550 nm and emission at 590 nm using the multimode reader Infinite M200 TECAN.

For ATP quantification, the CellTiter-Glo® Luminescent Cell Viability (Promega, Madison, WI, USA) assay was used. First, the 96-well plate containing Fx treated cells was left at room temperature for 30 min. Then, cells were incubated with CellTiter-Glo® reagents in an orbital shaker for 2 min. Next, the plate was acclimated for 10 min for stabilization of the luminescent signal and the total luminescence was evaluated with a Spectramax Paradigm multimode reader.

Scanning electron microscopy. Scanning electron microscopy (SEM) was utilized to observe the effect of Fx on the cell surface morphology. GBM1 cells were seeded on coverslips overnight and exposed to 100 μM of Fx for 24 h. After incubation, cells were fixed with PFA 4% for 20 min, and post-fixed with osmium tetroxide 1% for 2 h. Afterwards, cells were rinsed in 0.1 M cacodylate buffer and dehydrated in a graded acetone series (30-100%) for 10 min. The coverslips containing the cells were attached on top of the stubs using double-sided carbon tape and then dried using a carbon dioxide critical point dryer (Leica EM CPD030). Next, they were coated with gold using an ionic sputter coater (Leica EM SCD 500). They were then viewed and photographed by scanning electron microscopy using JEOL JSM-6390 LV Scanning Electron Microscope (Central Laboratory of Electron Microscopy/UFSC).

Transmission electron microscopy. Transmission electron microscopy (TEM) was used to analyze the GBM1 cell ultrastructural characteristics after exposure to Fx. This experiment was based on a previous study (43). First, GBM1 cells were seeded into 25 cm^2 culture flasks, and after they reached confluency, treated with or without 100 μ M Fx for 24 h. The GBM1 cells were then fixed for 24 h with 2.5% glutaraldehyde and 0.1 mol/l sodium cacodylate buffer (pH 7.2-7.4). Afterwards, the cell suspensions were washed three times with a cacodylate buffer and post-fixed with 1% osmium tetroxide (EMS) in a 0.1 mol/l sodium cacodylate buffer, at room temperature for 2 h. Next, the cells were incubated with increasing series of acetone (10 min each), for dehydration, and with a series of acetone and Spurr's resin (EMS) infiltration, followed by two infiltrations in pure resin (12 h each). The sample was then cut in ultrathin sections (80 nm) that were placed on copper wire mesh grids. Then, the samples were air-dried, incubated with uranyl acetate (2.0%, for 15 min) and reincubated with lead citrate (1% for 15 min). Subsequently, the sections were analyzed and images were taken with a JEM-1011 (Jeol) transmission electron microscope (Central Laboratory of Electron Microscopy/UFSC).

HUVEC chemotactic migration assay. To analyze the anti-angiogenic activity of Fx, a chemotactic migration assay was performed, using a Transwell® chamber as described previously (44). First, GBM1 cells were seeded on a 24-well plate overnight. After the HUVECs were detached, resuspended (1×10^6 cells/ml) and placed (100 μl) on the upper chamber of the Transwell®. Next, the Transwell® was placed on a GBM1 24-well plate. The lower chamber medium was then replaced with DMEM-F12 containing different concentrations of Fx (600 μl). The plate was cultivated at 37˚C in a humidified incubator with 5% CO_2 for 24 h. After incubation, the non-migrated cells were detached using a cotton-tip. The cells located on the bottom of the Transwell® were fixed and stained for 10 min with Hoechst (5 μg/ml). The membrane was divided in 4 quarters (0.8 cm diameter) each corresponding to one visual field under the microscope; the cells in each quarter were counted and photographed (Zeiss Axiovert 40 CFL, capture system AxioCam MRc).

In vitro endothelial tube formation assay. To evaluate the effect of Fx on HUVEC differentiation, a tube formation assay was carried out according to previous studies (45). HUVECs are the most studied human endothelial cell type, because this cell line is not difficult to isolate and culture. They also provide an optimal model for angiogenic *in vitro* studies because they differentiate and form vessel tubes (46). First, a 96-well plate was coated with Matrigel® for 30 min to allow polymerization. Then, HUVECs were seeded on the coated well (1×10^5 cells/ml) and incubated for 12 h with the condition media of GBM1 cells treated with Fx (100 μM). After incubation, tube formation was analyzed and images were taken using an inverted phase contrast microscope (Zeiss Axiovert 40 CFL, capture system AxioCam MRc). The acquired images were analyzed using ImageJ®.

Ex ovo angiogenesis assay using quail vitelline membrane. The induction of angiogenesis is one of the most important tumorigenic mechanisms (47). Therefore, a quail vitelline membrane assay was performed to evaluate the antiangiogenic activity of Fx in GBM cells. This assay was based on the development of a vascular system in the vitelline membrane. First, fertilized quail (*Coturnix japonica)* eggs were placed in a humidified egg incubator for 2 days at 38˚C. Then, the eggshells were gently opened and the embryos and the yolks were transferred to a 12-well plate so that the yolk-sac blood vessels facing upward. Next, a filter paper soaked with conditioned supernatant medium of Fx treated or untreated GBM cells were placed on the vitelline membrane precisely near the main right vein. The plates were then cultured in a standard humidified cell culture incubator at 37˚C, for 1 day. Afterwards, images of the embryos and the capillaries underneath the filter paper were captured with a microscope (Olympus MVX10, capture system Olympus cell Sens Entry 1.16). To evaluate the Fx anti-angiogenic effect, the number of vessels under the filter paper were counted and divided by the area of the paper, the number of capillaries diverging around it were also quantified using the ImageJ® software. Fibroblast growth factor-2 (FGF_2, Sigma-Aldrich) was used for the proangiogenic control group.

Statistical analysis. Statistical analysis was performed by one-way analysis of variance (ANOVA) followed by a Student-Newman-Keuls test. The data were expressed as the mean and standard deviation, considering a significance level of $p<0.05$. The software used to analyze the results and create the graphs was GraphPad Prism 7.0.

Results

Fucoxanthin decreases human glioblastoma cell viability. The cytotoxicity effect of Fx against GBM1 cells was evaluated using the MTT assay (Figure 1A). Fx showed cytotoxic activity against all the glioblastoma cell lines tested (GBM1, A172 and C6), after treatment for 24 h at concentrations over 70 μM. The Fx 100 μM concentration decreased GBM1, A172 and C6 viability, by an average of 66%, 42% and 50% respectively. However, 10 μM Fx increased the viability of GBM1 and A172 (32% and 12%, respectively). When exposed to 100 and 150 μM Fx, the number the GBM1 Hoechst positive cells significantly decreased around 60% and 40%, respectively (Figures 1C, D). Furthermore, the Fx cytotoxicity effect on non-tumorigenic cells was evaluated using a primary culture of murine astrocytes (Figure 1B). The results revealed that the viability of astrocytes also significantly increased at 10 μM Fx (23%) and decreased only when exposed to 150 μM Fx (40%). With 150 μM Fx, the number of Hoechst positive astrocytes also decreased

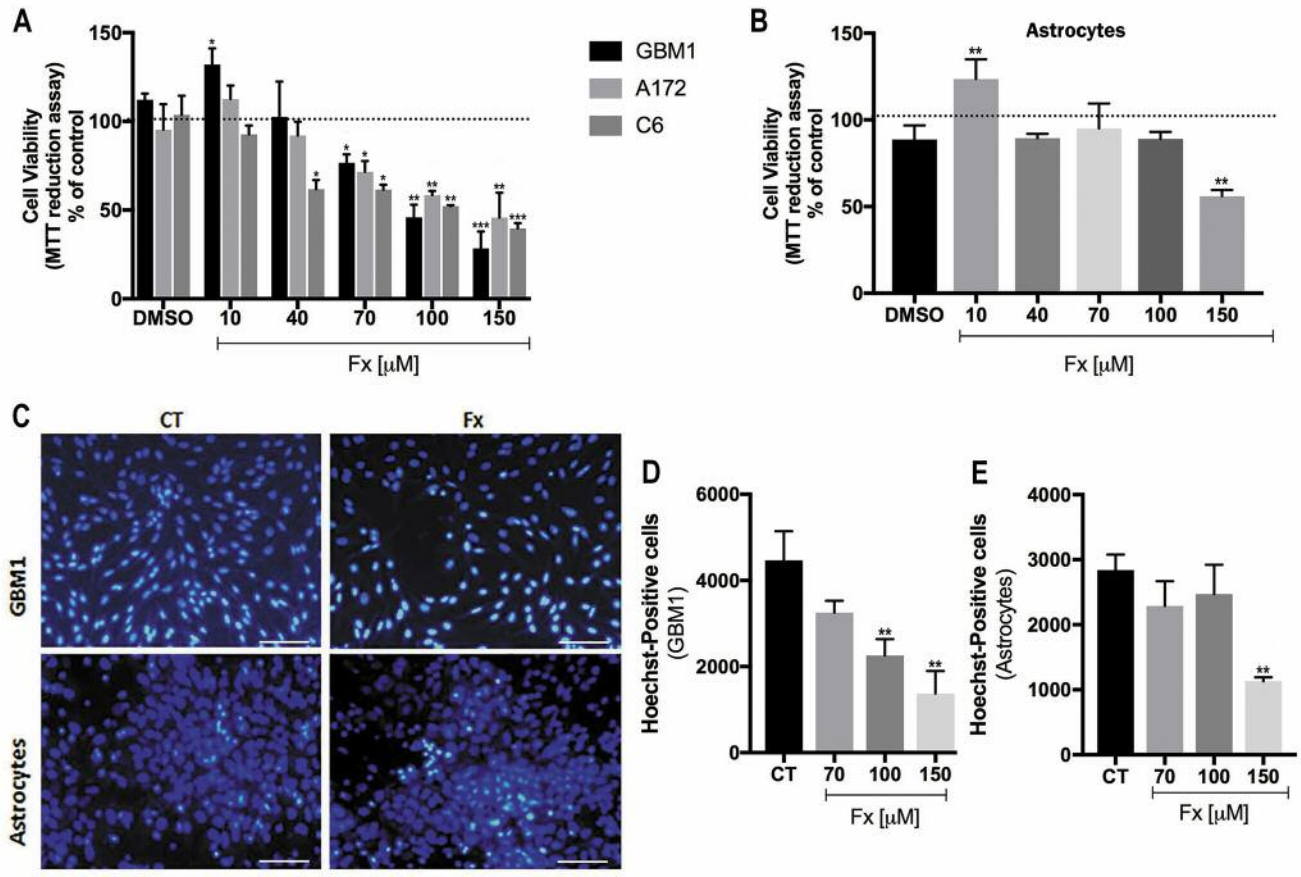

Figure 1. *Fucoxanthin decreased glioblastoma cell viability. A) GBM1, A172, C6 and, B) murine cortical astrocytes were treated with Fucoxanthin (10-150 mM) or vehicle (DMSO) in DMEM-F12. Cell viability was accessed by the MTT assay after 24 h. Data were expressed as percentage of cell viability versus the control group (dotted line) from four independent experiments performed in triplicates. C) The nuclei of GBM1 and murine cortical astrocytes were stained by Hoechst after Fucoxanthin (70-150 μM) treatment for 24 h and counted. Twelve fields randomly chosen (n=3) were analyzed in each experiment. D) Graphic representation of GBM1 cells and E) astrocytes evaluated by ImageJ® software. All viability data are expressed as the mean±standard deviation. *p<0.05; **p<0.01; ***p<0.001 representing a significant difference compared to the control group (one-way ANOVA followed by the Newman Keuls test). Bars=50 μm.*

approximately 40% compared with the control (Figure 1C, E). Treatment with DMSO (vehicle) did not affect cell viability. For the following assays, only the GBM1 lineage and the concentrations of 40, 70 and 100 μM of Fx were used. The 150 μM concentration was not used for further experiments due to its cytotoxicity to non-tumorigenic cells.

Fucoxanthin inhibits the proliferation and clonogenic potential of human glioblastoma cells. A Ki-67 cell proliferation assay was performed to investigate the Fx-proliferation activity on GBM1 cells (Figure 2A). Through this assay, we determined that the number of proliferating Ki-67-positive GBM1 cells was 45% lower in the Fx 100 μM treated cells compared to the control cells (Figure 2B).

In order to complement the analysis of the Fx anti-proliferative effect on GBM1 cells, the clonogenic and replicative potential of a single Fx-treated GBM1 cell was assessed through a clonogenic assay (Figure 2C). The results demonstrated that cells treated with 70 or 100 μM of Fx had lower percentage viability than the control cells (≈55% and 33% respectively), indicating that the number of clones at the end of the 12th day was lower in Fx-pre-exposed cells than in control cells (Figure 2D).

Fucoxanthin decreases cell migration and invasion of human glioblastoma cells. The Fx effect on GBM1 cell migration was analyzed by the wound-healing and Transwell assays. The wound-healing assay results (Figure 3A) indicated that GBM1 cells treated with 40 μM Fx migrated more slowly from the wound edge than control cells. In contrast, cells treated with 70 or 100 μM Fx did not migrate at all, the length of the scratch after 24 h was the same as at 0 h. At 0 h, there was no

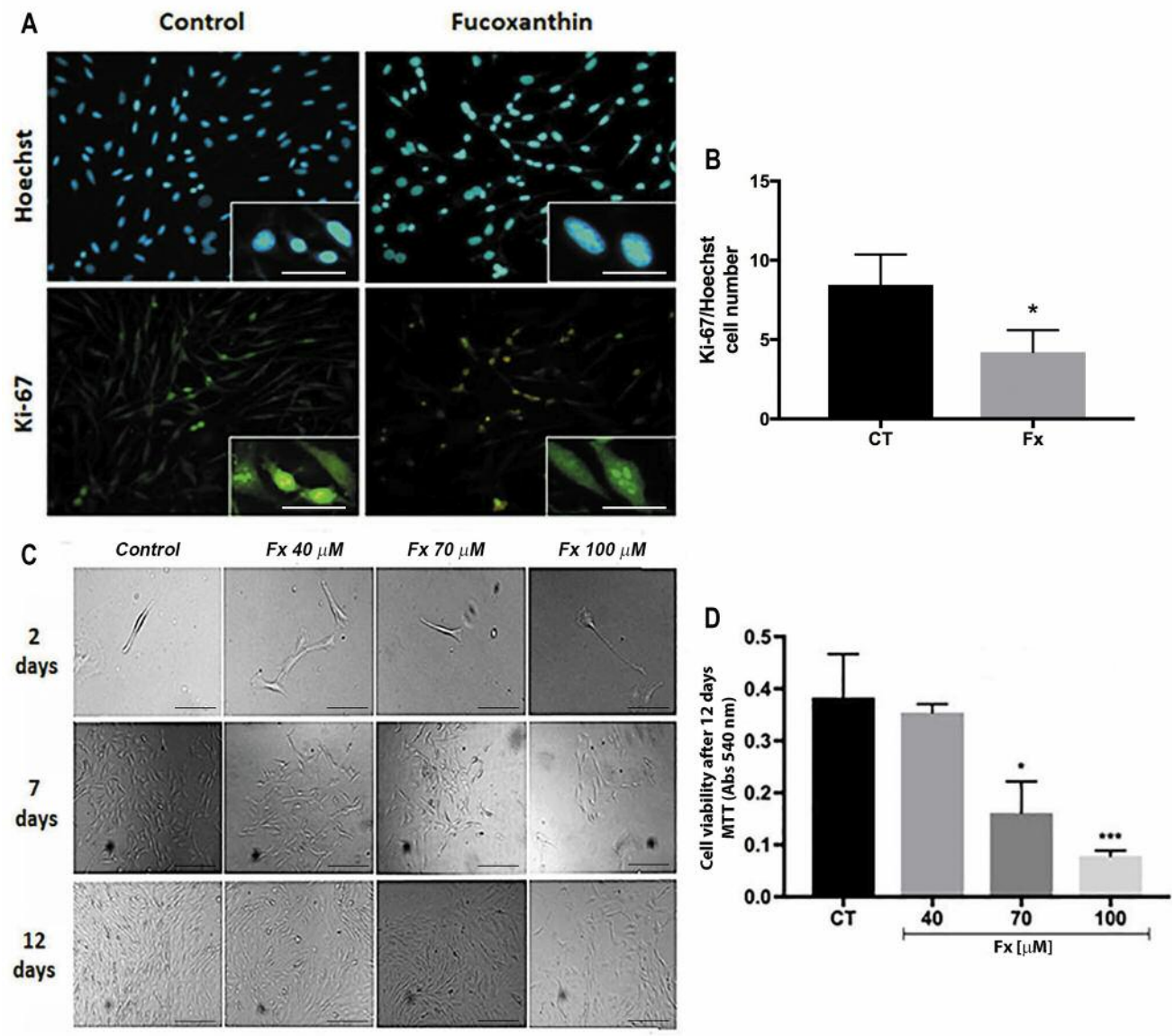

Figure 2. *Fucoxanthin reduced proliferation and clonogenic potential of human glioblastoma cells. A) After fucoxanthin treatment (100 μM) for 24 h, Ki-67 was performed to evaluate the cell proliferation (green: Ki-67-positive; blue: Hoechst nuclei staining). Ten randomly pictures were chosen from each group and analyzed by ImageJ® software. B) Graphic representation of GBM1 cell proliferation. Quantification was performed by dividing the number of Ki-67-positive cells by the total number of cells (Hoechst stained) in all groups. C) The GBM1 cells proliferative potential was accessed by single cell colony formation. After 24 h of fucoxanthin treatment (40-100 μM) cells were trypsinized, counted and 1 cell per well was seeded. Ten random fields were analyzed for each condition at 2, 7 and 12 days. D) GBM1 viability was assayed by MTT assay at the 12th day of incubation. The proliferation data are expressed as the mean±standard deviation of three independent experiments. *p<0.05; ***p<0.001 representing a significant difference compared to the control group (one-way ANOVA followed by the Newman Keuls test). Bars=50 μm.*

difference among the groups of cells (Figure 3B). Similar results were obtained from the Transwell® migration assay (Figure 3C). GBM1 cells exposed to different Fx concentrations (40, 70 or 100 μM) migrated less than the control cells. In the 100 μM Fx-treated cells, the number of cells that migrated through the insert was approximately 70% lower compared to the control cells (Figure 3D). To mimic cell invasion on the extracellular matrix, a Transwell® coated with Matrigel® assay was performed (Figure 3E). The results suggested that the number of GBM1 cells invading the Matrigel® remarkably decreased after Fx treatment. The number of GBM1 cells that invaded the Matrigel® when

exposed to 40, 70 and 100 μM Fx was 85%, 87% and 90%, respectively, lower than the control cells (Figure 3F).

Fucoxanthin induced apoptosis in human glioblastoma cell line. To evaluate if the Fx-cytotoxic effect on glioblastoma cells was associated with apoptosis or necrosis induction, a flow cytometry assay was performed. As shown in Figure 4 (A, B), the percentage of apoptotic GBM1 cells was significantly elevated when exposed to Fx (100 μM). The percentage of cells undergoing late or early apoptosis after Fx exposure was 46% higher compared to the control cells. Fx did not increase PI incorporation levels in GBM1 cells compared to control cells, demonstrating absence of necrosis. Next, the Fx effect on GBM1 mitochondrial function and morphology was investigated. The GBM1 mitochondrial membrane potential ($\Delta\Psi m$) maintenance was evaluated with a TMRE assay. According to the results, untreated GBM1 cells elicited maximal TMRE fluorescence, which reflects intact functional mitochondria. The Fx (100 μM) treatment resulted in a dissipation of $\Delta\Psi m$, detected by a consequent decrease in mean fluorescence. $\Delta\Psi m$ was reduced by 41% when cells were treated with Fx (Figure 4C). The GBM1 mitochondria's function was also indirectly measured, through quantification of ATP levels. After treatment with 100 μM Fx for 24 h, ATP levels were estimated using CellTiter 96® AQueous One Solution (MTS) assay. The different Fx concentrations decreased the ATP levels in GBM1 cells. The ATP levels were reduced 33%, 84% and 89% on cells exposed to Fx 40, 70 and 100 μM, respectively, when compared with the control cells (Figure 4D). In addition, ETM images showed significant ultrastructural changes in Fx-treated GBM1 cells. After treatment, cells presented apoptotic morphological features and exhibited aberrant mitochondria, disruption of cristae and blebbing of the internal mitochondrial membrane (Figure 4F). Ultrastructural alterations were also observed in the endoplasmic reticulum (ER) (Figure 4H). In the control, GBM1 cells showed normal ultrastructure of mitochondria and ER (Figures 4E, G).

To observe the nuclear morphology and confirm apoptotic cell features, a Hoechst 33258 staining assay was assessed. As shown in Figure 5A, control cells presented normal round shape cellular nuclei with a uniform low-density fluorescence distribution. Fx treated cells (100 μM) presented nuclear morphological alternation such as chromatin condensation and fragmentation with more concentrated and high-density fluorescence nuclei compared to untreated cells (Figure 5B). Apart from Hoechst staining, Fx effects on GBM1 cell nuclei were also examined using ETM. Untreated cells display a normal nuclei ultrastructure, and evenly distributed chromatin (Figure 5C). In contrast, after Fx exposure, GBM1 cells presented significant nuclei ultrastructural changes, including chromatin margination and condensation (Figure 5D).

The morphological cellular effects, induced by Fx (100 μM) on GBM1 were also analyzed by SEM. The analysis revealed significant morphological cellular alterations in GBM1 cells after Fx treatment (100 μM) compared to the control cells. The untreated cells had smooth, finite, and rigid surface areas with good cell membrane integrity (Figures 5E, F). In contrast, when corroborating the results previously mentioned, cells exposed to Fx presented significant cell membrane deformations, including a decrease in the number of microvilli, blebs and apoptotic bodies formation (Figures 5G, H). In addition, the extracellular matrix (ECM) of GBM1 cells exposed to Fx was dramatically altered. In comparison with the control cells, ECM from Fx-treated cells suffered intensive degradation and deformation.

Fucoxanthin inhibits endothelial differentiation in vitro. The angiogenesis induction is one of the hallmarks of cancer. Therefore, the Fx effect on the chemotactic migration of HUVECs was evaluated by a Transwell® assay (Figure 6A). The Fx treatment (40, 70 and 100 μ M) did not prevent the migration of HUVECs. The number of migrated-HUVEC cells in the presence of Fx was the same as in the control group (Figure 6B). Next, in order to examine the endothelial differentiation *in vitro,* an endothelial tube formation assay was also performed. The conditioned medium of GBM1 treated cells (Fx 100 μM) significantly inhibited tubulogenesis (Figure 6C); however, tube formation occurred in the control group. In contrast, in the group exposed to the Fx-treated GBM1 conditioned medium no tubular structure was formed, only clusters assembled by HUVEC cells.

Conditioned medium of cells treated with Fucoxanthin inhibits angiogenesis in vivo. In order to further investigate the Fx anti-angiogenic activity on GBM cells, an *ex-ovo* angiogenesis assay using quail vitelline membrane was performed (Figure 7A). Figure 7A, B shows a decreased vascularization of the yolk membrane at the group containing the conditioned medium of Fx-treated cells. In contrast, there was no difference among the number of vessels per filter area between the control groups (conditioned medium control, DMEM-F12 and FGF_2). In addition, the vascularization surrounding the filter was also analyzed (Figure 7C). A significant decrease in the number of vessels that diverged from the insert was observed in the group containing the conditioned medium of Fx-treated GBM1 cells. Likewise, there was no difference between the control groups on the diverged vascularization.

Our results show that fucoxanthin affects cancer cell processes, such as proliferation, migration/invasion, extracellular matrix distribution, apoptosis and angiogenesis.

Discussion

Despite the recent advances in research, no significant progress has been made towards preventing the lethality of high-grade gliomas. Therefore, there is a continuing need for

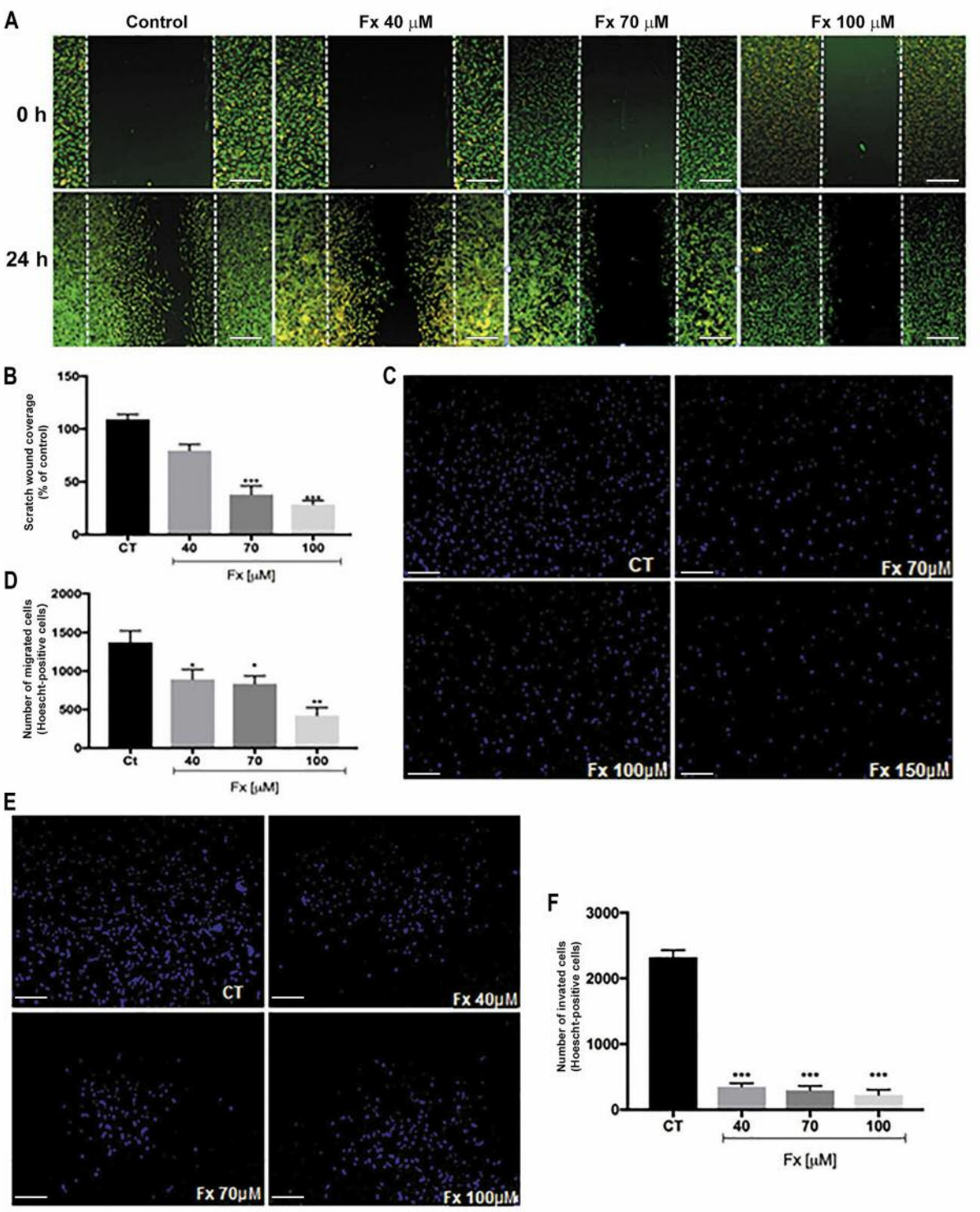

Figure 3. *Fucoxanthin decreased cell migration and invasion of human glioblastoma cells. After 24 h of fucoxanthin treatment (40 – 100 μM), GBM1 cell migration/invasion was evaluated by three different assays. A) Wound-healing protocol at 0 and 24 h of migration. Cells were stained with acridine orange dye. B) Gap width was quantified as arbitrary units of pixel number on ImageJ® software, of three independent experiments. C) Representative image of Hoechst positive cells that migrated through the insert of the Transwell® after 24 h of migration. D) Graphic representation of the migrated cell number, counted in ten random fields from each Transwell® insert, of three independent experiments. E) Transwell® inserts were coated with Matrigel® where the GBM1 cells were seeded. The analysis was made after 24 h (blue: Hoechst-positive GBM1 cells invading). F) Graphic quantification of GBM1 cell invasion in Matrigel®. Ten random fields were counted in each of the three replicates. *p<0.05; **p<0.01; ***p<0.001 representing a significant difference compared to the control group (one-way ANOVA followed by the Newman Keuls test). Bars=50 μm.*

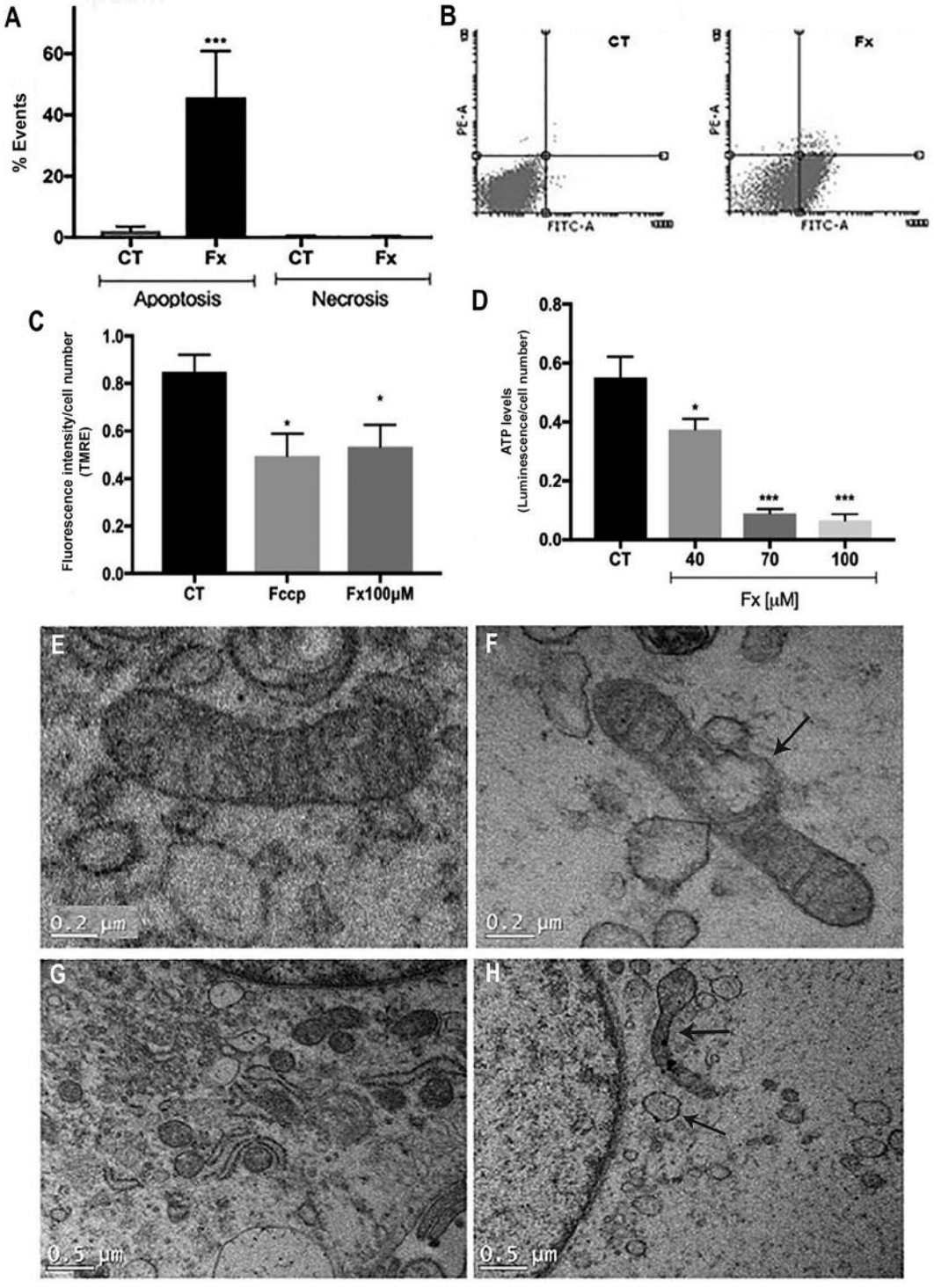

Figure 4. *Fucoxanthin induced apoptosis in human glioblastoma cell line. A) Graphic representation of flow cytometry for annexin V/propidium iodide assay on GBM1 cells after 24 h of fucoxanthin (100 μM) treatment. B) Illustrative dot plot of flow cytometry. C) GBM1 cells were also incubated with TMRE. The graph shows mitochondrial membrane depolarization induced by fucoxanthin (100 μM). D Graphic representation of ATP levels measured in GBM1 cells after fucoxanthin (100 μM) treatment. Data in (A), (B) and (D) are expressed as means±standard deviation of three independent experiments carried out in triplicates. *p<0.05; ***p<0.001 representing a significant difference compared to the control group. (E) TEM representative image of mitochondria of GBM1 control group and (F) of mitochondria of GBM1 cells treated with fucoxanthin- (100 μM) (black arrow indicates ruptured and abnormal mitochondrial membranes). (G) TEM representative image of endoplasmic reticulum (ER) of the control group and (H) of the ER of the group exposed to fucoxanthin (100 μM) (black arrows indicate swollen areas of the ER).*

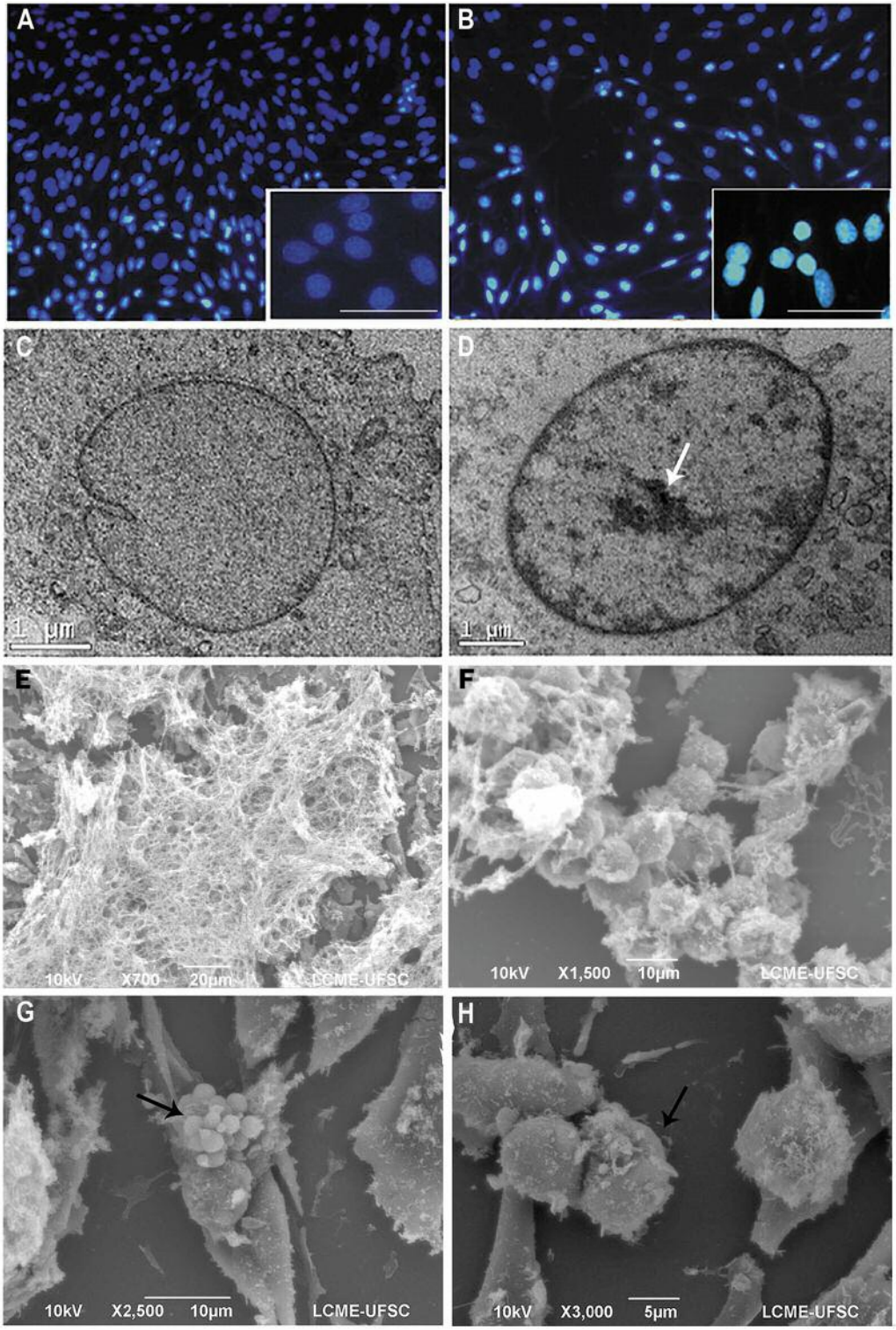

Figure 5. *Fucoxanthin promoted ultrastructural alteration and extracellular matrix in human remodeling in glioblastoma cell line. A) Representative images of Hoechst staining of nuclei of control and, B) Fucoxanthin-treated GBM1 cells. Insert shows pyknotic nuclei after fucoxanthin (100 μM) treatment for 24 h. C) TEM representative image of nuclei of a control GBM1 cell and (D) a Fucoxanthin-treated (100 μM) cell, with features that correspond to densely packed nucleus and chromatin condensation (white arrow). E) SEM representative image of control GBM1 cells, with spindle-shaped cells and dense extracellular matrix (ECM). F, G, H) SEM representative image of fucoxanthin-treated (100 μM) cells presenting apoptotic bodies (black arrows) and ECM morphological alterations and degradation.*

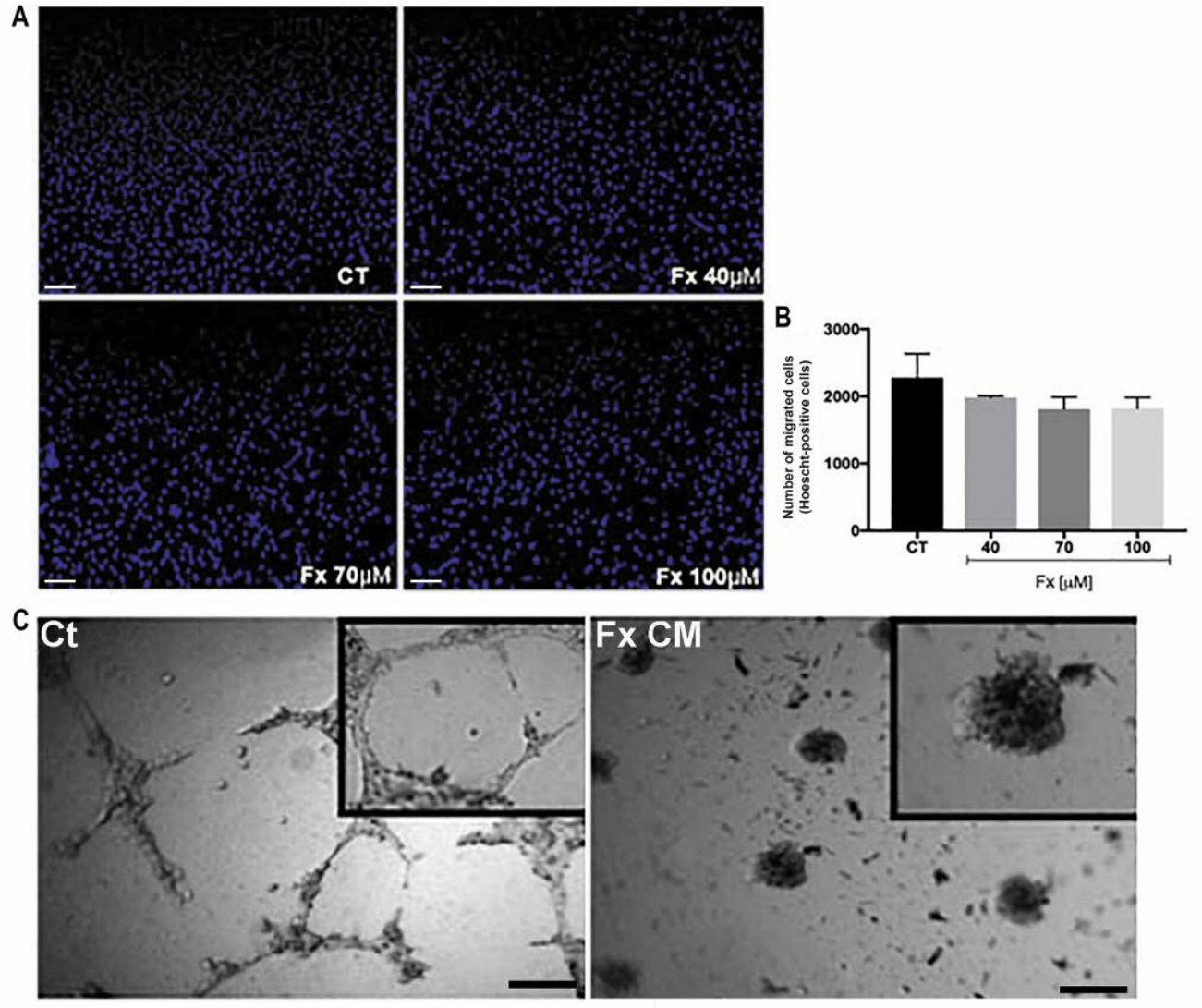

Figure 6. *Fucoxanthin inhibited endothelial differentiation in vitro. The HUVEC cells migration and differentiation were tested. A) Representative picture of the Transwell® coated with Matrigel® containing HUVEC cells (Hoechst staining) on top of the GBM1 cells treated for 24 h with fucoxanthin (40-100 μM). Bars=50 μM. B) Graphic representation of the HUVEC Transwell® assay. Data are expressed as the mean percentages of migration±standard deviation of three independent experiments and analyzed by one-way ANOVA followed by the Newman Keuls test. C) Representative images of HUVECs cultured on Matrigel® and GBM1-treated (fucoxanthin 100 μM) conditioned medium for 16 h and observed under a phase contrast microscope. Left insert: Tube formation by HUVEC treated with control GBM1 cells conditioned medium. Right insert: HUVECs exposed to conditioned medium from fucoxanthin-treated GBM1 cells, forming only cell clusters. Bars=100 μm.*

an effective treatment that has few side effects and promotes cytotoxicity on GBM cells. Fx can be an excellent option, as it is an abundant natural carotenoid, found in edible macro algae that exhibits diverse biological activities, such as cytotoxicity against several neoplasm cell lines (22, 28-34).

Several studies have demonstrated that Fx induces significant effects on different cancer cells including a concentration-dependent cytotoxicity (22, 28-34). In colorectal and lung cancer cells, Fx decreased significantly viability at concentrations above 20 μM following treatment for 24 h (20, 35). In bladder cancer, Fx decreased cell viability at concentrations above 40 μM after treatment for 24 h (48). In liver cancer, the cell viability decreased at 25 and 50 μM Fx in 24 and 48 h (49). Furthermore, several studies have demonstrated that tumor cells were affected more than non-tumorigenic cells, indicating that Fx has cytotoxicity effects on different cell lines, targeting almost exclusively cancer cells (29, 50-53).

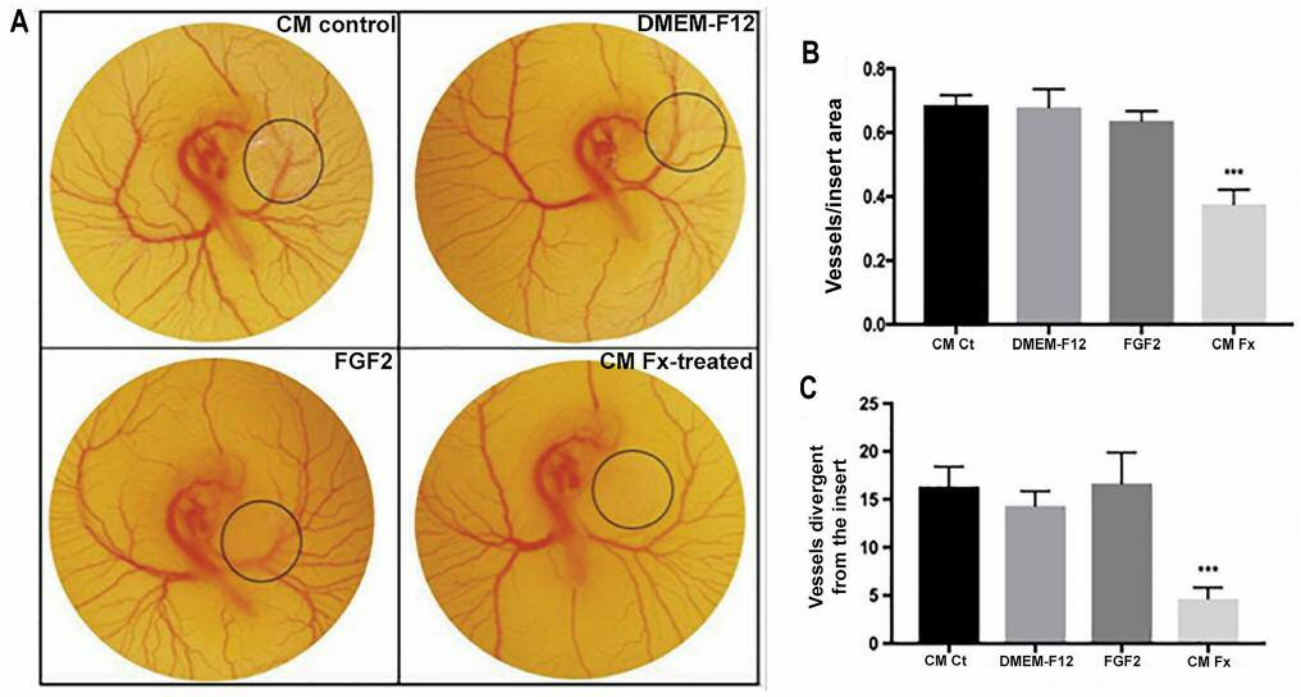

Figure 7. *Conditioned medium of fucoxanthin treated-GBM cells inhibited angiogenesis in vivo. Angiogenic ex ovo assay, carried out with a filter paper soaked with conditioned medium of fucoxanthin-treated GBM1 cells (100 μM) or control cells, DMEM-F12 and DMEM-F12 + FGF2 (as positive control). The filters were placed on the vitelline membrane near the right main vein. A) After 24 h the quail embryos were photographed and the capillaries underneath the filter paper and the vessels that diverged from it were counted. B) Graphic representation of the number of vessels under the filter paper diveded by the area of the paper for each group. C) Graphic representation of the number of vessels that diverged from the filter. Data are expressed as the means±standard deviation and four embryos were analyzed for each group. All filters were placed in the same position in the embryo yolk membrane. ***p<0.001 representing a significant difference compared to the control group (one-way ANOVA followed by the Newman Keuls test).*

In this study, the marine carotenoid Fx exhibited a concentration-dependent cytotoxic effect on human glioblastoma cell lines (GBM1 and A172) and on a rat glioma cell line (C6) at concentrations up to 70 μM, while had not affect normal the murine astrocytes. Furthermore, it was observed that Fx (70 μM and 100 μM) induced a greater cytotoxic effect on GBM1 compared to similar concentrations of TMZ (data not shown), one of the most widely used drug in the treatment of glioblastoma (54, 55).

Several studies have demonstrated that Fx induced an anti-proliferative effect in numerous types of tumors (29, 50-53). In this work, Fx exhibited anti-proliferative activity at a concentration (100 μM at 24 h) higher than that tested in other carcinoma types. Despite the impressive cytotoxic effect, Fx treatment did not cause the death of all GBM1 cells, considering that approximately 30% of the cells survived the treatment. These remaining cells are probably glioma stem cells (GSCs), giving the fact that they are highly present in the tumor cellular niche, their capacity for self-renewal, clonogenic activity, and resistance to drugs (56-58). Likewise, no studies have demonstrated an anti-clonogenic Fx activity in tumor cells. This study demonstrated that Fx decreased the number of clones and the proliferative activity of GBM1 cells. These results indicate that Fx treatment did not eliminate all GBM1 cells. However, the remaining cells proliferated less and more slowly, which could consequently lead to a tumorigenic regression.

The poor prognosis for GBM is due to a series of factors, including the high capacity of tumor cell invasion. The GBM high recurrence rate is mostly due to the ability of tumor cells to migrate and invade the healthy tissue. These cell mechanisms result in multifocal lesions reducing the efficiency of traditional therapies. These cancer cells can migrate into normal brain tissue where they evade surgery or radiation therapy (59-61). Therefore, there is a compelling need to establish a new treatment option that can suppress GBM cell mobility mechanisms. Fx had demonstrated anti-invasive activity in carcinogenic strains (27, 62). In metastatic murine melanoma cells (B16-F10), Fx treatment decreased the number of invasive B16-F10 cells as well as the secretion levels and expression of matrix metalloproteinase-9 (MMP-9), a protein that can degrade type IV collagen during tumor invasion (62).

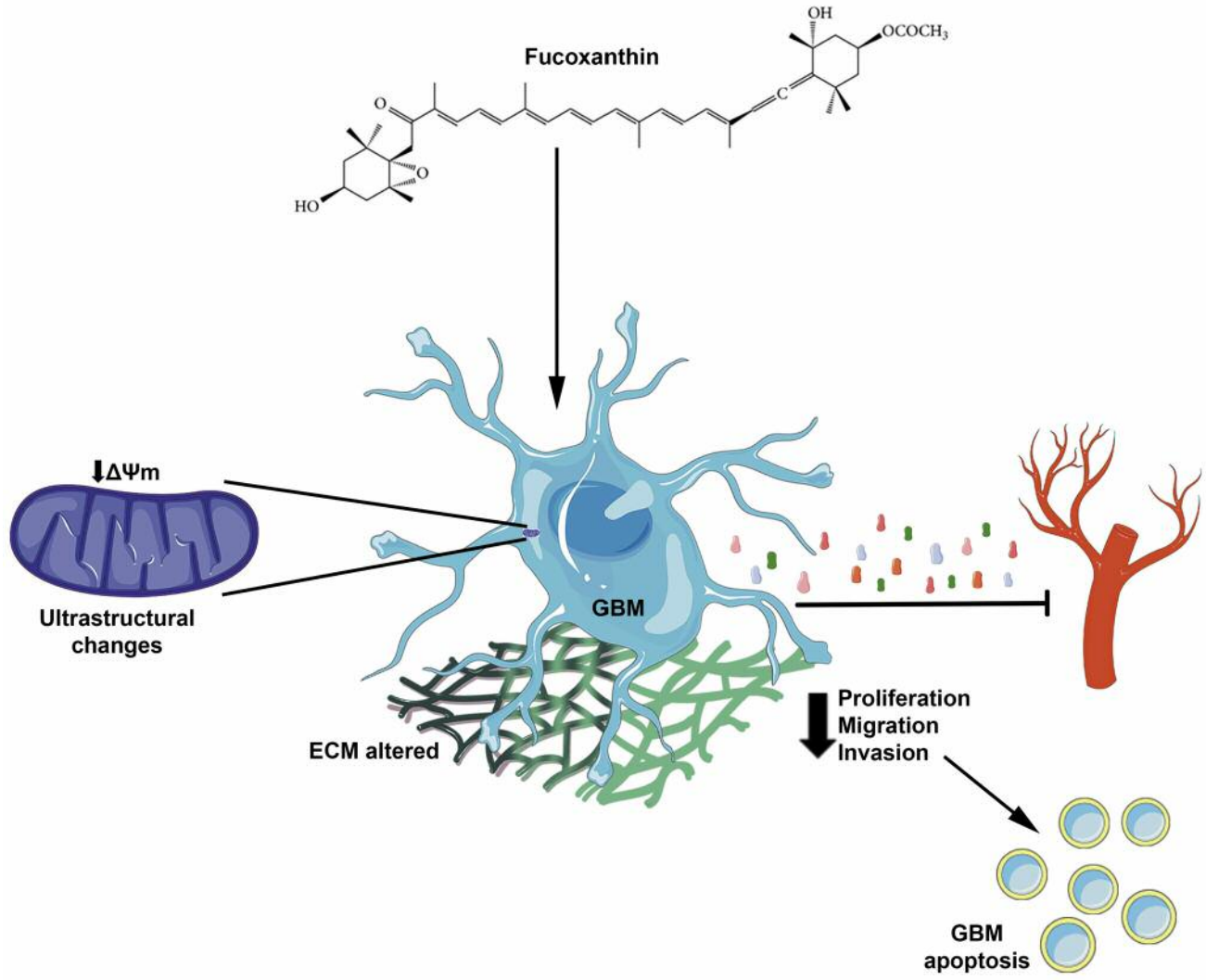

Figure 8. *Schematic model of fucoxanthin effects on GBM1 cells. Fucoxanthin decreases mitochondrial membrane potential, promotes ultrastructural alterations and remodeling of extracellular matrix. In addition, fucoxanthin-treated GBM1 cells release factors that inhibit angiogenesis. Consequently, processes involved in tumorigenesis such as proliferation, migration, and invasion are reduced, leading the GBM1 cells to apoptosis. This figure was produced using Servier Medical Art (80).*

The present study showed that GBM cells exposed to Fx (at concentrations up to 40 μM) migrated and invaded less than the control group. Similar results were obtained by Liu and colleagues (27); Fx treatment (50 μM) decreased the migration and invasion and of U87 and U251 glioblastoma cell lines *via* MMP-2 and MMP-9 inhibition.

In addition to cellular mobility mechanisms and tissue remodeling, angiogenesis is a dominant mechanism that impacts tumor progression (63, 64). Studies have demonstrated that germinal angiogenesis is an essential process for the growth of tumors beyond 2-3 mm in size (65). Thus, the inhibition of this process could suppress tumor progression. Previous studies have shown that many marine-derived substances can display inhibitory effects on new vessel development (66). This work showed that Fx failed to prevent HUVEC migration in the presence of GBM1 cells. These results indicated that this carotenoid did not prevent the release of growth factors by GBM1 cells, which attracted the endothelial cells, or that Fx served as a chemoattractant for these types of cells. Furthermore, we observed that the conditioned medium of the Fx-treated GBM1 cells prevented tubule formation, indicating that Fx-GBM1 treatment could prevent the differentiation of endothelial cells. Moreover, the *ex ovo* anti-angiogenic assay results showed that the conditioned medium of Fx-treated GBM1 cells decreased both yolk quail membrane vascularization and branch formation.

However, we cannot assert that the anti-angiogenic effects observed were due solely to the lack of angiogenic factors in the conditioned medium of cells treated with Fx or exclusively to the presence of this carotenoid. These results are in agreement with the results obtained by Sugawara and colleagues (50). They discovered that Fx was able to suppress the differentiation of endothelial progenitor cells, reduce the endothelial cells tube's length and impair the *neovessel* formation, with no particular effect on the chemotaxis of HUVEC cells. Therefore, the results obtained in this study reinforced the benefits of using Fx as an alternative treatment for GBM. Nevertheless, the molecular pathway of the Fx anti-angiogenic effects requires future studies.

Another characteristic of the resistant and aggressive GBM is its capacity for apoptosis evasion. Deregulation of apoptosis is a key event that contributes to tumor development; thus, induction of apoptosis can be a strategy for cancer treatment (15, 67, 68). Recent studies have indicated that Fx induced apoptosis in different cancer cell lines; for instance, Zhang and colleagues (69) showed that Fx promoted apoptosis in EJ-1 urinary bladder cancer cells. Apoptosis may be associated with morphological changes, DNA laddering, activation of the caspase-3 and increased number of hypodiploid cells. Kotake-Nara and collaborators (30) have demonstrated that Fx induced loss of HL-60 mitochondrial membrane potential associated with an increase of the apoptosis levels and did not alter the reactive oxygen species levels.

Our work data demonstrated that Fx induced apoptosis in GBM1 and did not increase the levels of necrosis. This effect was considered positive because necrosis might significantly impair the survival rates of glioma patients but it can be a histological factor that promotes the progression of a malignant astrocytoma to GBM (70).

The early stage of the intrinsic apoptosis pathway is marked by mitochondrial membrane permeabilization followed by the loss of membrane potential inducing the release of proapoptotic proteins, including AIF and cytochrome to cytosol (71-73). Likewise, we also detected that Fx treatment decreased the mitochondrial membrane potential and the levels of intracellular ATP, and induced modifications in the structure of mitochondria in GBM1. This suggests that the apoptotic effect of Fx is associated with the reduction of $\Delta\Psi m$, and subsequently, with the induction of the apoptosis intrinsic pathway. Therefore, the effect of Fx on mitochondria and the consequent apoptosis induction mechanism deserve future investigation.

The extracellular matrix (ECM) has a crucial role in tumor progression. Tumors often display an altered ECM protein organization (74). In normal tissue, ECM regulates basic cell mechanisms such as cell mobility, growth, survival and differentiation. In tumors, ECM actively contributes to their histopathology and behavior. Tumor tissue is usually stiffer compared to the normal tissue. In a tumorigenic environment, cells proliferate more when they interact with a stiffer ECM due to a response to the growth factors (75-77). This environment stimulates the expression of Erk, P13K and Rac (75, 78, 79). This work was the first to demonstrate the effect of Fx on glioblastoma cell ECM. The results indicated that Fx was able to alter the ECM of GBM1 cells. The SEM images suggested that Fx exposure induced ECM degradation and morphological alterations, which is considered another positive effect for alternative glioblastoma treatment. Nevertheless, additional studies are necessary to confirm this hypothesis.

Conclusion

In conclusion, fucoxanthin is a potent inducer of apoptosis, with anti-proliferative, anti-invasion and anti-angiogenic properties in glioblastoma cells. Together, these alterations may explain the antitumoral effects on GBM1 cells (Figure 8). However, further studies are needed to elucidate the complete cellular and molecular anti tumorigenic mechanisms of fucoxanthin in glioblastoma cells.

Conflicts of Interest

All Authors declare no conflicts of interest regarding this study.

Authors' Contributions

Conceptualization: Flávia Garcia Lopes, Karen Andrinéia Oliveira, Rafael Garcia Lopes, Carla Inês Tasca and Cláudia Beatriz Nedel. Methodology: Flávia Garcia Lopes, Karen Andrinéia Oliveira, Carmen Simioni, Gabriel da Silva Pescador, Ricardo Castilho Garcez, Gabriela Poluceno and Cláudia Marlene Bauer. Validation: Flávia Garcia Lopes, Karen Andrinéia Oliveira, Carla Inês Tasca, Cláudia Beatriz Nedel. Formal Analysis: Flávia Garcia Lopes and Cláudia Beatriz Nedel. Investigation: Flávia Garcia Lopes. Resources: Rafael Garcia Lopes, Carmen Simioni, Cláudia Marlene Bauer, Marcelo Maraschin, Roberto Bianchini Derner, Ricardo Castilho Garcez, Carla Inês Tasca and Cláudia Beatriz Nedel. Supervision: Carla Inês Tasca and Cláudia Beatriz Nedel. Writing – Original Draft Preparation: Flávia Garcia Lopes, Rafael Garcia Lopes and Cláudia Beatriz Nedel. Writing – Review & Editing: Flávia Garcia Lopes, Karen Andrinéia Oliveira, Rafael Garcia Lopes, Carla Inês Tasca and Cláudia Beatriz Nedel; Visualization: Flávia Garcia Lopes; Project Administration: Flávia Garcia Lopes, Carla Inês Tasca and Cláudia Beatriz Nedel.

Acknowledgements

The Authors would like to thank the technicians of the Laboratório Multiusuários de Estudos em Biologia (LAMEB/CCB/UFSC) and of the Laboratório Central de Microscopia Eletrônica (LCME/UFSC) for their assistance in the standard analyses.

Funding

This study was supported by grants from the Brazilian funding agencies Conselho Nacional de Desenvolvimento Científico e

Tecnológico (CNPq), Instituto Nacional de Ciência e Tecnologia/ CNPq, Coordenação de Aperfeiçoamento de Pessoal de Ensino Superior (CAPES) and CAPES-PVE 052.

References

1 Ferris SP, Hofmann JW, Solomon DA and Perry A: Characterization of gliomas: From morphology to molecules. Virchows Arch *471(2)*: 257-269, 2017. PMID: 28674742. DOI: 10.1007/s00428-017-2181-4

2 Bondy ML, Scheurer ME, Malmer B, Barnholtz-Sloan JS, Davis FG, Il'yasova D, Kruchko C, McCarthy BJ, Rajaraman P, Schwartzbaum JA, Sadetzki S, Schlehofer B, Tihan T, Wiemels JL, Wrensch M, Buffler PA and Consortium BTE: Brain tumor epidemiology: Consensus from the brain tumor epidemiology consortium. Cancer *113(7 Suppl)*: 1953-1968, 2008. PMID: 18798534. DOI: 10.1002/cncr.23741

3 Ostrom QT, Gittleman H, Stetson L, Virk SM and Barnholtz-Sloan JS: Epidemiology of gliomas. Cancer Treat Res *163:* 1-14, 2015. PMID: 25468222. DOI: 10.1007/978-3-319-12048-5_1

4 Ostrom QT, Gittleman H, Liao P, Vecchione-Koval T, Wolinsky Y, Kruchko C and Barnholtz-Sloan JS: Cbtrus statistical report: Primary brain and other central nervous system tumors diagnosed in the united states in 2010-2014. Neuro Oncol *19(suppl_5)*: v1-v88, 2017. PMID: 29117289. DOI: 10.1093/neuonc/nox158

5 Ohgaki H and Kleihues P: Genetic alterations and signaling pathways in the evolution of gliomas. Cancer Sci *100(12)*: 2235-2241, 2009. PMID: 19737147. DOI: 10.1111/j.1349-7006.2009.01308.x

6 Tamimi AF and Juweid M: Epidemiology and outcome of glioblastoma. *In*: Glioblastoma [internet]. S DV (ed.). Codon Publications: Brisbane (AU), 2017.

7 Wen PY and Kesari S: Malignant gliomas in adults. N Engl J Med *359(5)*: 492-507, 2008. PMID: 18669428. DOI: 10.1056/NEJMra0708126

8 Xu H, Chen J and Qin Z: Geographic variations in the incidence of glioblastoma and prognostic factors predictive of overall survival in us adults from 2004-2013. Front Aging Neurosci *9:* 352, 2017. PMID: 29163134. DOI: 10.3389/fnagi.2017.00352

9 Ohgaki H and Kleihues P: Epidemiology and etiology of gliomas. Acta Neuropathol *109(1)*: 93-108, 2005. PMID: 15685439. DOI: 10.1007/s00401-005-0991-y

10 Wesseling P, Kros JM and Jeuken JWM: The pathological diagnosis of diffuse gliomas: Towards a smart synthesis of microscopic and molecular information in a multidisciplinary context. Diagn Histopathol *17(11)*: 486-494, 2011. DOI: 10.1016/j.mpdhp.2011.08.005

11 Stupp R, Taillibert S, Kanner A, Read W, Steinberg DM, Lhermitte B, Toms S, Idbaih A, Ahluwalia MS, Fink K, Di Meco F, Lieberman F, Zhu JJ, Stragliotto G, Tran DD, Brem S, Hottinger AF, Kirson ED, Lavy-Shahaf G, Weinberg U, Kim CY, Paek SH, Nicholas G, Burna J, Hirte H, Weller M, Palti Y, Hegi ME and Ram Z: Effect of tumor-treating fields plus maintenance temozolomide *vs* maintenance temozolomide alone on survival in patients with glioblastoma: A randomized clinical trial. JAMA *318(23)*: 2306-2316, 2017. PMID: 29260225. DOI: 10.1001/jama.2017.18718

12 Stupp R, van den Bent MJ and Hegi ME: Optimal role of temozolomide in the treatment of malignant gliomas. Curr Neurol Neurosci Rep *5(3)*: 198-206, 2005. PMID: 15865885. DOI: 10.1007/s11910-005-0047-7

13 Iacob G and Dinca EB: Current data and strategy in glioblastoma multiforme. J Med Life *2(4)*: 386-393, 2009. PMID: 20108752.

14 Hanif F, Muzaffar K, Perveen K, Malhi SM and Simjee SU: Glioblastoma multiforme: A review of its epidemiology and pathogenesis through clinical presentation and treatment. Asian Pac J Cancer Prev *18(1)*: 3-9, 2017. PMID: 28239999. DOI: 10.22034/APJCP.2017.18.1.3

15 Krakstad C and Chekenya M: Survival signalling and apoptosis resistance in glioblastomas: Opportunities for targeted therapeutics. Mol Cancer *9:* 135, 2010. PMID: 20515495. DOI: 10.1186/1476-4598-9-135

16 Wilson TA, Karajannis MA and Harter DH: Glioblastoma multiforme: State of the art and future therapeutics. Surg Neurol Int *5:* 64, 2014. PMID: 24991467. DOI: 10.4103/2152-7806.132138

17 Hou LC, Veeravagu A, Hsu AR and Tse VC: Recurrent glioblastoma multiforme: A review of natural history and management options. Neurosurg Focus *20(4)*: E5, 2006. PMID: 16709036. DOI: 10.3171/foc.2006.20.4.2

18 Demuth T and Berens ME: Molecular mechanisms of glioma cell migration and invasion. J Neurooncol *70(2)*: 217-228, 2004. PMID: 15674479. DOI: 10.1007/s11060-004-2751-6

19 Das S and Marsden PA: Angiogenesis in glioblastoma. N Engl J Med *369(16)*: 1561-1563, 2013. PMID: 24131182. DOI: 10.1056/NEJMcibr1309402

20 Mei C, Zhou S, Zhu L, Ming J, Zeng F and Xu R: Antitumor effects of laminaria extract fucoxanthin on lung cancer. Mar Drugs *15(2)*, 2017. PMID: 28212270. DOI: 10.3390/md15020039

21 Dembitsky VM, Gloriozova TA and Poroikov VV: Natural peroxy anticancer agents. Mini Rev Med Chem *7(6)*: 571-589, 2007. PMID: 17584156. DOI: 10.2174/138955707780859396

22 Peng J, Yuan JP, Wu CF and Wang JH: Fucoxanthin, a marine carotenoid present in brown seaweeds and diatoms: Metabolism and bioactivities relevant to human health. Mar Drugs *9(10)*: 1806-1828, 2011. PMID: 22072997. DOI: 10.3390/md9101806

23 Maeda H, Hosokawa M, Sashima T, Funayama K and Miyashita K: Effect of medium-chain triacylglycerols on anti-obesity effect of fucoxanthin. J Oleo Sci *56(12)*: 615-621, 2007. PMID: 17992001. DOI: 10.5650/jos.56.615

24 Jeon SM, Kim HJ, Woo MN, Lee MK, Shin YC, Park YB and Choi MS: Fucoxanthin-rich seaweed extract suppresses body weight gain and improves lipid metabolism in high-fat-fed c57bl/6j mice. Biotechnol J *5(9)*: 961-969, 2010. PMID: 20845386. DOI: 10.1002/biot.201000215

25 Nishino H, Murakosh M, Ii T, Takemura M, Kuchide M, Kanazawa M, Mou XY, Wada S, Masuda M, Ohsaka Y, Yogosawa S, Satomi Y and Jinno K: Carotenoids in cancer chemoprevention. Cancer Metastasis Rev *21(3-4)*: 257-264, 2002. PMID: 12549764. DOI: 10.1023/a:1021206826750

26 Kim KN, Heo SJ, Yoon WJ, Kang SM, Ahn G, Yi TH and Jeon YJ: Fucoxanthin inhibits the inflammatory response by suppressing the activation of nf-κb and mapks in lipopolysaccharide-induced raw 264.7 macrophages. Eur J Pharmacol *649(1-3)*: 369-375, 2010. PMID: 20868674. DOI: 10.1016/j.ejphar.2010.09.032

27 Liu Y, Zheng J, Zhang Y, Wang Z, Yang Y, Bai M and Dai Y: Fucoxanthin activates apoptosis *via* inhibition of pi3k/akt/mtor pathway and suppresses invasion and migration by restriction of p38-mmp-2/9 pathway in human glioblastoma cells. Neurochem Res *41(10)*: 2728-2751, 2016. PMID: 27394418. DOI: 10.1007/s11064-016-1989-7

28 Hosokawa M, Kudo M, Maeda H, Kohno H, Tanaka T and Miyashita K: Fucoxanthin induces apoptosis and enhances the antiproliferative effect of the ppargamma ligand, troglitazone, on colon cancer cells. Biochim Biophys Acta *1675(1-3)*: 113-119, 2004. PMID: 15535974. DOI: 10.1016/j.bbagen.2004.08.012

29 Moreau D, Tomasoni C, Jacquot C, Kaas R, Le Guedes R, Cadoret JP, Muller-Feuga A, Kontiza I, Vagias C, Roussis V and Roussakis C: Cultivated microalgae and the carotenoid fucoxanthin from Odontella aurita as potent anti-proliferative agents in bronchopulmonary and epithelial cell lines. Environ Toxicol Pharmacol *22(1)*: 97-103, 2006. PMID: 21783694. DOI: 10.1016/j.etap.2006.01.004

30 Kotake-Nara E, Terasaki M and Nagao A: Characterization of apoptosis induced by fucoxanthin in human promyelocytic leukemia cells. Biosci Biotechnol Biochem *69(1)*: 224-227, 2005. PMID: 15665492. DOI: 10.1271/bbb.69.224

31 Kotake-Nara E, Kushiro M, Zhang H, Sugawara T, Miyashita K and Nagao A: Carotenoids affect proliferation of human prostate cancer cells. J Nutr *131(12)*: 3303-3306, 2001. PMID: 11739884. DOI: 10.1093/jn/131.12.3303

32 Das SK, Hashimoto T, Shimizu K, Yoshida T, Sakai T, Sowa Y, Komoto A and Kanazawa K: Fucoxanthin induces cell cycle arrest at g0/g1 phase in human colon carcinoma cells through up-regulation of p21waf1/cip1. Biochim Biophys Acta *1726(3)*: 328-335, 2005. PMID: 16236452. DOI: 10.1016/j.bbagen.2005.09.007

33 Zhang H, Tang Y, Zhang Y, Zhang S, Qu J, Wang X, Kong R, Han C and Liu Z: Fucoxanthin: A promising medicinal and nutritional ingredient. Evid Based Complement Alternat Med *2015:* 723515, 2015. PMID: 26106437. DOI: 10.1155/2015/723515

34 Okuzumi J, Nishino H, Murakoshi M, Iwashima A, Tanaka Y, Yamane T, Fujita Y and Takahashi T: Inhibitory effects of fucoxanthin, a natural carotenoid, on n-myc expression and cell cycle progression in human malignant tumor cells. Cancer Lett *55(1)*: 75-81, 1990. PMID: 2245414. DOI: 10.1016/0304-3835(90)90068-9

35 Takahashi K, Hosokawa M, Kasajima H, Hatanaka K, Kudo K, Shimoyama N and Miyashita K: Anticancer effects of fucoxanthin and fucoxanthinol on colorectal cancer cell lines and colorectal cancer tissues. Oncol Lett *10(3)*: 1463-1467, 2015. PMID: 26622691. DOI: 10.3892/ol.2015.3380

36 Mendes-de-Aguiar CB, Alchini R, Decker H, Alvarez-Silva M, Tasca CI and Trentin AG: Thyroid hormone increases astrocytic glutamate uptake and protects astrocytes and neurons against glutamate toxicity. J Neurosci Res *86(14)*: 3117-3125, 2008. PMID: 18543341. DOI: 10.1002/jnr.21755

37 Mosmann T: Rapid colorimetric assay for cellular growth and survival: Application to proliferation and cytotoxicity assays. J Immunol Methods *65(1-2)*: 55-63, 1983. PMID: 6606682. DOI: 10.1016/0022-1759(83)90303-4

38 Yelskaya Z, Carrillo V, Dubisz E, Gulzar H, Morgan D and Mahajan SS: Synergistic inhibition of survival, proliferation, and migration of u87 cells with a combination of ly341495 and iressa. PLoS One *8(5)*: e64588, 2013. PMID: 23724064. DOI: 10.1371/journal.pone.0064588

39 Naliwaiko K, Luvizon AC, Donatti L, Chammas R, Mercadante AF, Zanata SM and Nakao LS: Guanosine promotes b16f10 melanoma cell differentiation through pkc-erk 1/2 pathway. Chem Biol Interact *173(2)*: 122-128, 2008. PMID: 18456249. DOI: 10.1016/j.cbi.2008.03.010

40 Justus CR, Leffler N, Ruiz-Echevarria M and Yang LV: In vitro cell migration and invasion assays. J Vis Exp *88*, 2014. PMID: 24962652. DOI: 10.3791/51046

41 Bittencourt LF, Oliveira KA, Cardoso CB, Lopes FG, Dal-Cim T, Chiaradia-Delatorre LD, Mascarello A, Maluf SW, Yunes RA, Garcez RC, Tasca CI and Nedel CB: Novel synthetic chalcones induces apoptosis in human glioblastoma cells. Chem Biol Interact *252:* 74-81, 2016. PMID: 27012433. DOI: 10.1016/j.cbi.2016.03.022

42 Egea J, Rosa AO, Cuadrado A, García AG and López MG: Nicotinic receptor activation by epibatidine induces heme oxygenase-1 and protects chromaffin cells against oxidative stress. J Neurochem *102(6)*: 1842-1852, 2007. PMID: 17540012. DOI: 10.1111/j.1471-4159.2007. 04665.x

43 Costa CHD, Perreault F, Oukarroum A, Melegari SP, Popovic R and Matias WG: Effect of chromium oxide (iii) nanoparticles on the production of reactive oxygen species and photosystem ii activity in the green alga Chlamydomonas reinhardtii. Sci Total Environ *565:* 951-960, 2016. PMID: 26803219. DOI: 10.1016/j.scitotenv.2016.01.028

44 Zengel P, Ramp D, Mack B, Zahler S, Berghaus A, Muehlenweg B, Gires O and Schmitz S: Multimodal therapy for synergic inhibition of tumour cell invasion and tumour-induced angiogenesis. BMC Cancer *10:* 92, 2010. PMID: 20222943. DOI: 10.1186/1471-2407-10-92

45 DeCicco-Skinner KL, Henry GH, Cataisson C, Tabib T, Gwilliam JC, Watson NJ, Bullwinkle EM, Falkenburg L, O'Neill RC, Morin A and Wiest JS: Endothelial cell tube formation assay for the in vitro study of angiogenesis. J Vis Exp *91*: e51312, 2014. PMID: 25225985. DOI: 10.3791/51312

46 Morin KT and Tranquillo RT: *In vitro* models of angiogenesis and vasculogenesis in fibrin gel. Exp Cell Res *319(16)*: 2409-2417, 2013. PMID: 23800466. DOI: 10.1016/j.yexcr.2013.06.006

47 Hanahan D and Weinberg RA: The hallmarks of cancer. Cell *100(1)*: 57-70, 2000. PMID: 10647931. DOI: 10.1016/s0092-8674(00)81683-9

48 Wang L, Zeng Y, Liu Y, Hu X, Li S, Wang Y, Li L, Lei Z and Zhang Z: Fucoxanthin induces growth arrest and apoptosis in human bladder cancer t24 cells by up-regulation of p21 and down-regulation of mortalin. Acta Biochim Biophys Sin (Shanghai) *46(10)*: 877-884, 2014. PMID: 25187415. DOI: 10.1093/abbs/gmu080

49 Satomi Y and Nishino H: Implication of mitogen-activated protein kinase in the induction of g1 cell cycle arrest and gadd45 expression by the carotenoid fucoxanthin in human cancer cells. Biochim Biophys Acta *1790(4)*: 260-266, 2009. PMID: 19714865. DOI: 10.1016/j.bbagen.2009.01.003

50 Sugawara T, Baskaran V, Tsuzuki W and Nagao A: Brown algae fucoxanthin is hydrolyzed to fucoxanthinol during absorption by caco-2 human intestinal cells and mice. J Nutr *132(5)*: 946-951, 2002. PMID: 11983819. DOI: 10.1093/jn/132.5.946

51 Liu CL, Huang YS, Hosokawa M, Miyashita K and Hu ML: Inhibition of proliferation of a hepatoma cell line by fucoxanthin in relation to cell cycle arrest and enhanced gap junctional intercellular communication. Chem Biol Interact *182(2-3)*: 165-172, 2009. PMID: 19737546. DOI: 10.1016/j.cbi.2009.08.017

52 Matsumoto M, Hosokawa M, Matsukawa N, Hagio M, Shinoki A, Nishimukai M, Miyashita K, Yajima T and Hara H: Suppressive effects of the marine carotenoids, fucoxanthin and fucoxanthinol on triglyceride absorption in lymph duct-

cannulated rats. Eur J Nutr *49(4)*: 243-249, 2010. PMID: 19888619. DOI: 10.1007/s00394-009-0078-y

53 Yamamoto K, Ishikawa C, Katano H, Yasumoto T and Mori N: Fucoxanthin and its deacetylated product, fucoxanthinol, induce apoptosis of primary effusion lymphomas. Cancer Lett *300(2)*: 225-234, 2011. PMID: 21078541. DOI: 10.1016/j.canlet.2010.10.016

54 Messaoudi K, Clavreul A and Lagarce F: Toward an effective strategy in glioblastoma treatment. Part i: Resistance mechanisms and strategies to overcome resistance of glioblastoma to temozolomide. Drug Discov Today *20(7)*: 899-905, 2015. PMID: 25744176. DOI: 10.1016/j.drudis.2015.02.011

55 Wait SD, Prabhu RS, Burri SH, Atkins TG and Asher AL: Polymeric drug delivery for the treatment of glioblastoma. Neuro Oncol *17(Suppl 2):* ii9-ii23, 2015. PMID: 25746091. DOI: 10.1093/neuonc/nou360

56 Altaner C: Glioblastoma and stem cells. Neoplasma *55(5)*: 369-374, 2008. PMID: 18665745.

57 Bradshaw A, Wickremesekera A, Brasch HD, Chibnall AM, Davis PF, Tan ST and Itinteang T: Cancer stem cells in glioblastoma multiforme. Front Surg *3:* 48, 2016. PMID: 27617262. DOI: 10.3389/fsurg.2016.00048

58 Fedr R, Pernicová Z, Slabáková E, Straková N, Bouchal J, Grepl M, Kozubík A and Souček K: Automatic cell cloning assay for determining the clonogenic capacity of cancer and cancer stem-like cells. Cytometry A *83(5)*: 472-482, 2013. PMID: 23450810. DOI: 10.1002/cyto.a.22273

59 Sanai N and Berger MS: Glioma extent of resection and its impact on patient outcome. Neurosurgery *62(4)*: 753-764; discussion 264-756, 2008. PMID: 18496181. DOI: 10.1227/01.neu.0000318159. 21731.cf

60 Kim EH, Song HS, Yoo SH and Yoon M: Tumor treating fields inhibit glioblastoma cell migration, invasion and angiogenesis. Oncotarget *7(40)*: 65125-65136, 2016. PMID: 27556184. DOI: 10.18632/oncotarget.11372

61 Siebzehnrubl FA, Reynolds BA, Vescovi A, Steindler DA and Deleyrolle LP: The origins of glioma: E pluribus unum? Glia *59(8)*: 1135-1147, 2011. PMID: 21351156. DOI: 10.1002/glia.21143

62 Chung TW, Choi HJ, Lee JY, Jeong HS, Kim CH, Joo M, Choi JY, Han CW, Kim SY, Choi JS and Ha KT: Marine algal fucoxanthin inhibits the metastatic potential of cancer cells. Biochem Biophys Res Commun *439(4)*: 580-585, 2013. PMID: 24036125. DOI: 10.1016/j.bbrc.2013.09.019

63 Folkman J: Incipient angiogenesis. J Natl Cancer Inst *92(2)*: 94-95, 2000. PMID: 10639502. DOI: 10.1093/jnci/92.2.94

64 Nishida N, Yano H, Nishida T, Kamura T and Kojiro M: Angiogenesis in cancer. Vasc Health Risk Manag *2(3)*: 213-219, 2006. PMID: 17326328. DOI: 10.2147/vhrm.2006.2.3.213

65 Folkman J: Angiogenesis in psoriasis: Therapeutic implications. J Invest Dermatol *59(1)*: 40-43, 1972. PMID: 5039962. DOI: 10.1111/1523-1747.ep12625746

66 Yue PY, Leung HM, Li AJ, Chan TN, Lum TS, Chung YL, Sung YH, Wong MH, Leung KS and Zeng EY: Angiosuppressive properties of marine-derived compounds-a mini review. Environ Sci Pollut Res Int *24(10)*: 8990-9001, 2017. PMID: 26520098. DOI: 10.1007/s11356-015-5536-x

67 Pucci B, Kasten M and Giordano A: Cell cycle and apoptosis. Neoplasia *2(4)*: 291-299, 2000. PMID: 11005563. DOI: 10.1038/sj.neo.7900101

68 Gerl R and Vaux DL: Apoptosis in the development and treatment of cancer. Carcinogenesis *26(2)*: 263-270, 2005. PMID: 15375012. DOI: 10.1093/carcin/bgh283

69 Zhang Z, Zhang P, Hamada M, Takahashi S, Xing G, Liu J and Sugiura N: Potential chemoprevention effect of dietary fucoxanthin on urinary bladder cancer ej-1 cell line. Oncol Rep *20(5)*: 1099-1103, 2008. PMID: 18949407.

70 Raza SM, Lang FF, Aggarwal BB, Fuller GN, Wildrick DM and Sawaya R: Necrosis and glioblastoma: A friend or a foe? A review and a hypothesis. Neurosurgery *51(1)*: 2-12; discussion 12-13, 2002. PMID: 12182418. DOI: 10.1097/00006123-200207000-00002

71 Loeffler M and Kroemer G: The mitochondrion in cell death control: Certainties and incognita. Exp Cell Res *256(1)*: 19-26, 2000. PMID: 10739647. DOI: 10.1006/excr.2000.4833

72 Gottlieb E, Vander Heiden MG and Thompson CB: Bcl-x(l) prevents the initial decrease in mitochondrial membrane potential and subsequent reactive oxygen species production during tumor necrosis factor alpha-induced apoptosis. Mol Cell Biol *20(15)*: 5680-5689, 2000. PMID: 10891504. DOI: 10.1128/mcb.20.15.5680-5689.2000

73 Green DR and Kroemer G: The pathophysiology of mitochondrial cell death. Science *305(5684)*: 626-629, 2004. PMID: 15286356. DOI: 10.1126/science.1099320

74 Lu P, Weaver VM and Werb Z: The extracellular matrix: A dynamic niche in cancer progression. J Cell Biol *196(4)*: 395-406, 2012. PMID: 22351925. DOI: 10.1083/jcb.201102147

75 Provenzano PP, Inman DR, Eliceiri KW, Knittel JG, Yan L, Rueden CT, White JG and Keely PJ: Collagen density promotes mammary tumor initiation and progression. BMC Med *6:* 11, 2008. PMID: 18442412. DOI: 10.1186/1741-7015-6-11

76 Pickup MW, Mouw JK and Weaver VM: The extracellular matrix modulates the hallmarks of cancer. EMBO Rep *15(12)*: 1243-1253, 2014. PMID: 25381661. DOI: 10.15252/embr.201439246

77 Wells RG and Discher DE: Matrix elasticity, cytoskeletal tension, and tgf-beta: The insoluble and soluble meet. Sci Signal *1(10)*: pe13, 2008. PMID: 18334714. DOI: 10.1126/stke.110pe13

78 Provenzano PP and Keely PJ: Mechanical signaling through the cytoskeleton regulates cell proliferation by coordinated focal adhesion and rho gtpase signaling. J Cell Sci *124(Pt 8)*: 1195-1205, 2011. PMID: 21444750. DOI: 10.1242/jcs.067009

79 Bae YH, Mui KL, Hsu BY, Liu SL, Cretu A, Razinia Z, Xu T, Puré E and Assoian RK: A fak-cas-rac-lamellipodin signaling module transduces extracellular matrix stiffness into mechanosensitive cell cycling. Sci Signal *7(330)*: ra57, 2014. PMID: 24939893. DOI: 10.1126/scisignal.2004838

80 Servier Medical Art. Creative Commons, 2013. Available at: https://smart.servier.com/ [Last accessed May 5, 2020]

Received August 17, 2020
Revised October 8, 2020
Accepted October 9, 2020